

This manuscript is a preprint and has been submitted for publication in *Sedimentary Geology*. The manuscript has undergone peer-review, but subsequent versions of this manuscript may have different content. Please feel free to contact the first author directly regarding the manuscript. (brian.burnham@abdn.ac.uk)

Discriminating stacked distributary channel from palaeovalley fill sand bodies in foreland basin settings

Brian S. Burnham^{a,b}, Rhodri M. Jerrett^a, David Hodgetts^a, Stephen S. Flint^a

^a*Department of Earth and Environmental Sciences, University of Manchester, Manchester M13 9PL UK*

^b*School of Geosciences, Department of Geology and Geophysics, University of Aberdeen, Aberdeen AB24 3UE, UK*

Abstract

Stacked fluvial distributary channel deposits and palaeovalley fills can form major, multi-storey sand bodies with similar thicknesses, and with lateral extents often greater than a single exposure. Consequently, they can be difficult to tell apart from one another using outcrop data. This study addresses this problem by quantitatively analysing the architecture of five stacked fluvial distributary channel deposits and two palaeovalley fills from the Pennsylvanian Pikeville and Hyden formations of the central Appalachian Basin, USA. The *a priori* interpretation of the sand bodies as stacked distributary channels and palaeovalley fills is possible because a robust in-place coal seam correlation framework allows for the recognition of different basin-scale architectures for each type – aspect ratios <1000 and envelopes of fluvial and deltaic strata for stacked distributary channels, and aspect ratios >1000 and a regional basinward facies shift at the bases of palaeovalley fills. Sand body thickness, storey thickness, position and length of storey contacts within the sand body are similar in both types. However, they can be distinguished by different up-system to down-system changes in their respective architectures. Stacked distributary channel sand bodies thin down system, display a decrease in storey thickness, an increase in the mean position of storey heights in the sand body and a decrease in the length of storey contacts. These trends are the result of down-system decrease in channel size, and confinement associated with radially distributive fluvial systems. Palaeovalley fill sand bodies thicken down-system, display an increase in storey thickness, a decrease in the mean position of storey heights, and a decrease in the length of storey contacts. The increase in sand body and storey thickness are the result of down-system increases in original channel size, consistent with trunk axial fluvial systems fed by tributaries that predominate during valley-formation. The down-system increase in amalgamation reflects a down-system decrease in accommodation, from the higher subsidence rate active margin of the basin, and is therefore not necessarily characteristic of palaeovalley fill architectures in all basin settings. This study emphasises the requirement for detailed correlation work and quantitative analysis of external and internal architectures before the interpretation of sand bodies as stacked distributary channels or palaeovalley fills.

Keywords: 3D outcrop modelling, lidar, quantitative characterisation, Distributive Fluvial System, palaeovalley, foreland basin

Email address: brian.burnham@abdn.ac.uk (Brian S. Burnham)

1. Introduction

Major fluvial sand bodies which may be successions of stacked distributary channels (Hirst, 1992; Nichols and Fisher, 2007; Kukulski et al., 2013) or palaeovalley fills (e.g. Jennette et al., 1991; Hampson et al., 1999; Wu and Bhattacharya, 2015) have been the subject of extensive research because of their hydrocarbon reservoir potential. The difference between these two types of sand body is critical to the accurate prediction of reservoir geometry, for the correct reconstruction of palaeogeography, and sequence stratigraphic analysis. A challenge when discriminating between palaeovalley fills and stacked distributary channels at outcrop scales, is that the lateral extent of both sand body types commonly exceeds that of the exposure, and their respective thicknesses may be similar. Additionally, many incised valleys do not display a "basinward facies shift" at their base (Blum et al., 2013; Holbrook and Bhattacharya, 2012) – a key criterion historically used to identify palaeovalley fills (e.g. Posamentier and Vail, 1988; Van Wagoner et al., 1988, 1990). Recent studies of modern, active fluvial systems have shown that in plan view distributary fluvial channels bifurcate, and individual channel size decreases down-system (Hartley et al., 2010; Weissmann et al., 2010). By comparison, palaeovalleys are characterised by one axial fluvial system with a tendency for tributaries to converge into a major channel down-system (Blum et al., 2013). Therefore, in the stratigraphic record, the height of fully preserved storeys and thickness of the composite sand body should decrease down-system in stacked distributary channels. In palaeovalley fills, the opposite should be true: the thickness of fully preserved storeys and the thickness of the composite sand body should increase down-system. This criterion has been applied to the rock record to interpret distributive fluvial systems (Nichols and Fisher, 2007; Owen et al., 2015; Weissmann et al., 2013), but has not been rigorously applied as a means of recognising palaeovalley fills (c.f. Jerrett et al., 2017). In successions that contain both stacked distributary channels and palaeovalley fills, basin-wide up-dip to down-dip statistical trends in sand body size and preserved storey thickness may not be clear. To complicate matters further, full storey thicknesses are commonly not preserved within the sand bodies due to top-truncation by younger storeys, rendering palaeohydraulic analysis difficult. Nevertheless, the interpretation of fluvial sand bodies as either stacked distributary channels or palaeovalley fills should be possible via a detailed, quantitative analysis of the internal architecture and geometry of the sand body.

The majority of naturally-occurring rock exposures are markedly two dimensional (e.g., elongate coastal cliffs and road-cut exposures), presenting difficulties for the extraction of plan-view data, and reconstruction of fluvial style. However, advances over the past two decades in data collection, processing and analysis techniques have allowed for the quantitative description of the geostatistical properties of exposed successions, using three-dimensional (3D) digital outcrop models (DOMs) (Bellian et al., 2005; Buckley et al., 2008; Fabuel-Perez et al., 2010; Olariu et al., 2011; Hodgetts, 2013; Rarity et al., 2014; Burnham and Hodgetts, 2018). In this study, these digital geospatial and remote sensing approaches (i.e., lidar integration with coaxially aligned photography and differential geospatial navigation satellite system (DGNSS) measurements) have been applied to a succession of fluvial sand bodies from the Upper Carboniferous (Pennsylvanian) Breathitt Group of the central Appalachian Basin, USA (Fig. 1). The upper Breathitt Group contains fluvial sand bodies that are interpreted as progradational stacked distributary channels (Jerrett et al., 2017), and others that unequivocally represent palaeovalley fills, marked at their bases by regional basinward facies shifts of fluvial onto marine rocks (Aitken and Flint, 1994, 1995; Jerrett et al., 2017). The Breathitt Group therefore represents an ideal case study to achieve the key aims of this study. These are: (1) to quantitatively describe, and compare the architecture of stacked distributary channel and palaeovalley fill sand bodies, (2) determine principal depositional controls the resulting architectures, and (3) delineate criteria for the recognition of stacked distributary channels versus palaeovalley fills, from limited outcrop and subcrop data.

51 **2. Geological context**

52 The central Appalachian Basin (Fig. 1) was one of a series of Alleghenian-Variscan peripheral
 53 foreland depocentres that developed cratonward of promontories on the Laurasian continental
 54 margin during the collision of Gondwana with Laurasia in the late Palaeozoic (Thomas, 1976;
 55 Quinlan and Beaumont, 1984). In the Middle Carboniferous, initial thrust sheet emplacement
 56 along the southeast margin of Laurasia drove flexural subsidence of a pre-existing cratonic mixed
 57 clastic-carbonate shelf in present-day south eastern West Virginia, and western Virginia, and
 58 led to the formation of the SW-NE trending central Appalachian foreland basin (Quinlan and
 59 Beaumont, 1984; Tankard, 1986). The Central Appalachian Basin was filled by a Middle Car-
 60 boniferous to early Permian foreland megasequence up to 1.5 km thick on the SE margin of
 61 the basin, which overlapped older strata uplifting in the Cincinnati arch to the West (Fig. 1a),
 62 and a slowly subsiding platform north of the Irvine-Paint Creek (Figs. 1b), and the Kentucky
 63 River fault systems (Fig. 2a). The non-preservation of Carboniferous strata over the Cincinnati
 64 Arch (Fig. 1) makes it difficult to assess quite how far sediment accumulated on the NW cra-
 65 tonic margin of the basin, but present day exposures imply an (instantaneous) basin width, and
 66 commensurate lithospheric flexural wavelength of c. 100-200 km. The megasequence is broadly
 67 a coarsening-up succession of marine, marginal marine, terrestrial and lacustrine siliciclastics,
 68 coal and rare carbonates, in which evidence for marine conditions generally decreases upwards
 69 (Chesnut Jr, 1994; Horne et al., 1978). The basin was periodically flooded by marine transgres-
 70 sions from the SW, marked by marine mudstones along the axis of the basin. Clastic sediment
 71 was delivered via the normal and forced progradation of deltas and fluvial systems, sourced from
 72 the mature craton to the north and the uplifting Alleghanian Orogenic Belt to the SE. These
 73 deltas and the fluvial systems feeding them prograded axially (Aitken and Flint, 1994, 1995)
 74 and transversely (Jerrett et al., 2017) into the basin.

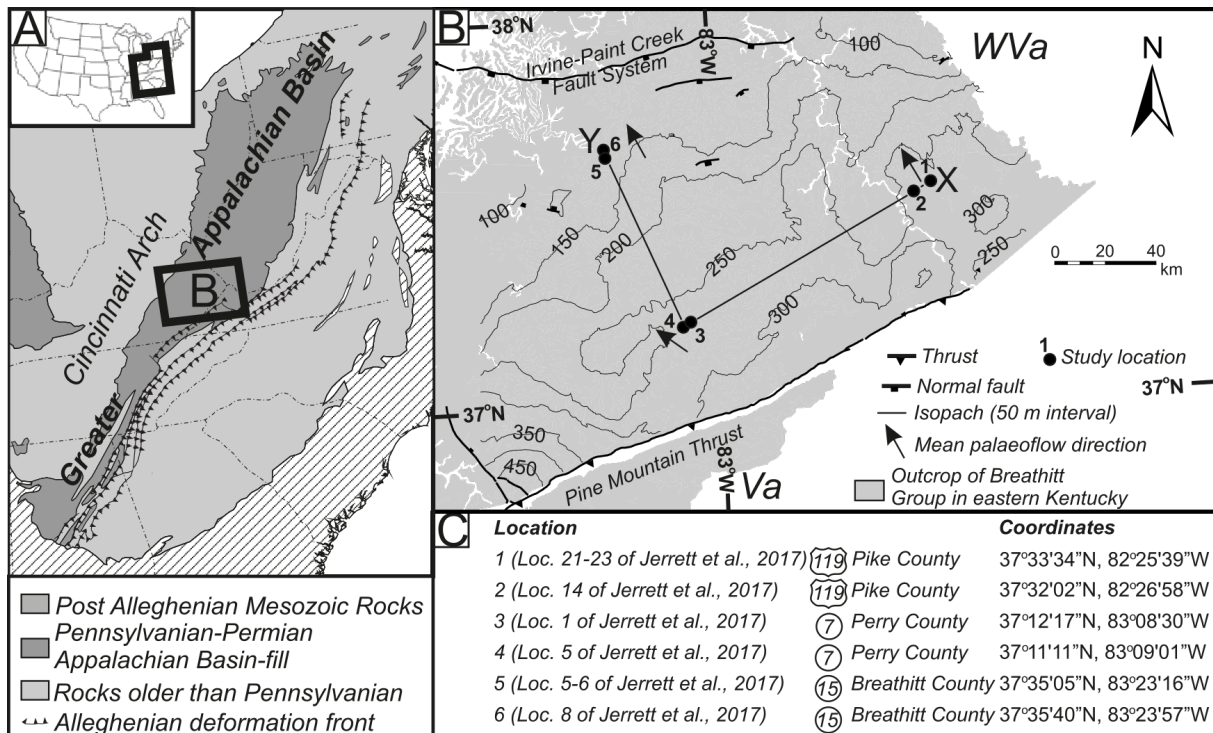


Figure 1: (A) Location of the study area in the contiguous USA and within the greater Appalachian Basin. (B) Geological map of eastern Kentucky, showing the location of the six road cuts which were targeted for study. Isopach lines of the combined thickness of the Pikeville and Hyden formations is shown, as well as vector mean palaeoflow measurements from the Pikeville and Hyden Formations (from Jerrett et al., 2017). Line of section X-Y in Figure 3 shown. (C) Location details of the six road cuts targeted for study. Abbreviations: Loc. = Location; Va = Virginia; WV = West Virginia.

75 The Pikeville and Hyden formations of the upper Breathitt Group are the targets of this study
 76 (Fig. 2). In outcrop, they contain major transversely oriented multi storey fluvial sand bodies

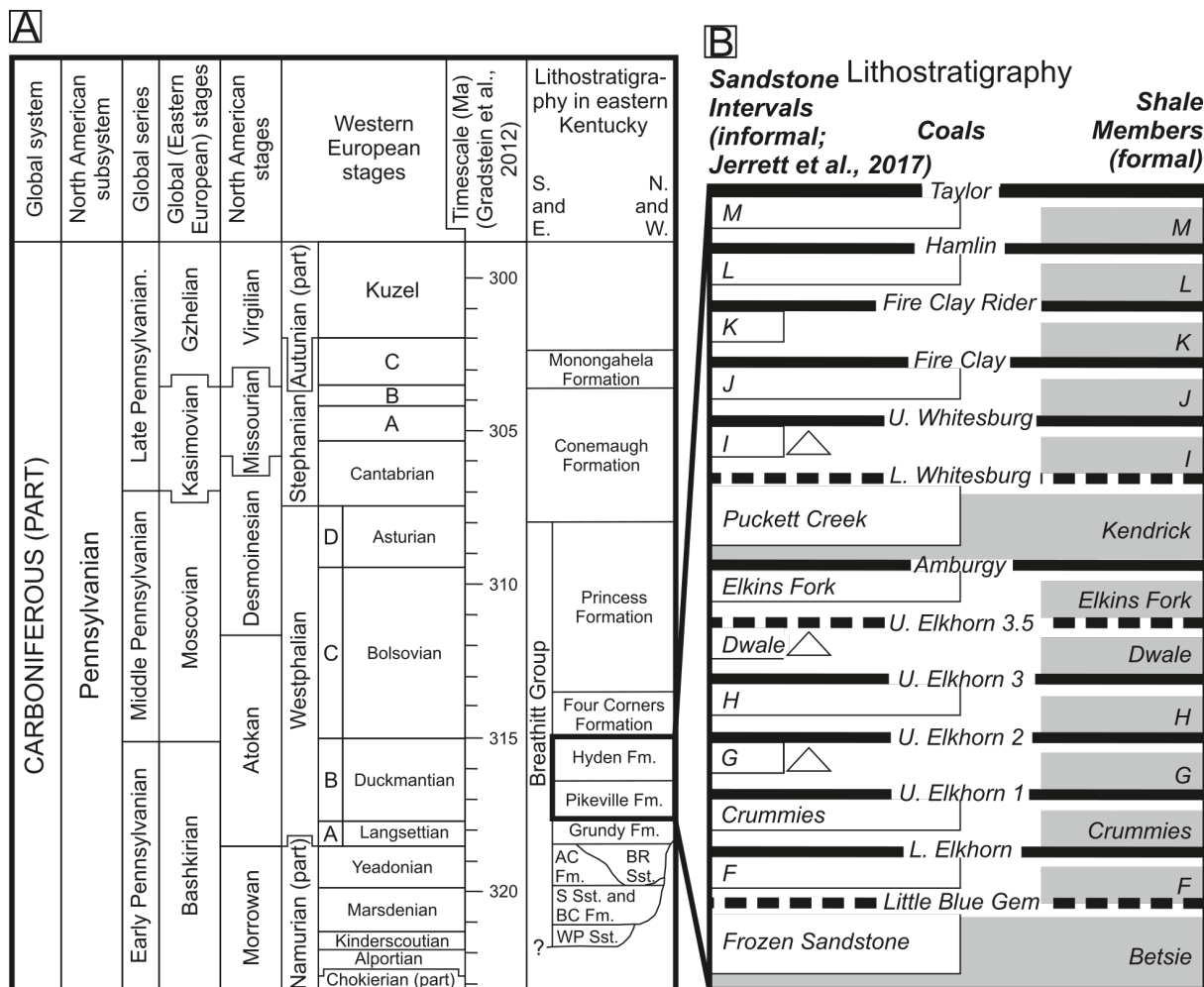


Figure 2: (A) Chronostratigraphy and lithostratigraphy of the Alleghanian foreland basin fill of the central Appalachian Basin in eastern Kentucky. Based on data from Greb et al. (2008), but recalibrated to the timescale of (Gradstein et al., 2012). Abbreviations: AC Fm. = Alvy Creek Formation; BC Fm. = Bottom Creek Formation; BR Sst. = Bee Rock Sandstone; WP Sst. = Warren Point Sandstone; S Sst. = Sewanee Sandstone. (B) Named coals, marine to marginal-marine shale members and fluvio-estuarine sandstone intervals in the Pikeville and Hyden formations (from Jerrett et al., 2017). Not all coals are shown, and dashed lines represent more locally developed coals (cf. Rice and Hiatt, 1994). More locally developed shale members, or those with equivocal evidence for deposition in fully marine conditions are shown in hatched grey. Width of speckled boxes corresponds to the basinward extent of the sandstone interval. These fluvio-estuarine sandstone intervals are the object of this study.

77 that can exceed 10 km wide, and are up to 40 m thick (Fig. 2b). Jerrett et al. (2017) noted that
 78 fluvial sand bodies incised into marine strata (regional basinward shifts in facies) also have aspect
 79 ratios greater than 1000, and that these represent palaeovalley fills. By contrast, sand bodies
 80 that show no basinward facies shifts anywhere in the basin have aspect ratios that are typically
 81 less than 1000. Jerrett et al. (2017) recognised that these sand bodies thin, or become absent
 82 down-system, and reasoned that they represent stacked successions of distributary channels
 83 which had distributed their sediment load across an aggrading delta plain. These authors also
 84 recognised an intermediate type of sand body with no evidence for a basinward facies shift up-
 85 dip, but do display a basinward shift in facies down-dip. These bodies have been interpreted
 86 as stacked distributary channels in the up-dip high accommodation orogenic part of the basin,
 87 but pass down-dip into palaeovalleys towards the more degradational, lower accommodation
 88 cratonic margin of the foreland basin. These sand bodies display intermediate aspect ratios to
 89 the two other types of multi storey fluvial sand bodies (Jerrett et al., 2017) and are not targeted
 90 for analysis in this study. All sand body types are extensively exposed in a series of road cuts
 91 constructed throughout eastern Kentucky since the 1970s (e.g. Horne et al., 1978; Chesnut Jr,
 92 1994; Aitken and Flint, 1995; Jerrett et al., 2017). Road cuts provided exposures up to 200

93 m high and 1 km long, but compared to the width of many of the sand bodies, irrespective of
94 genetic type, they are often too short to provide complete cross sections through the sand bodies,
95 capturing their complete external geometries and internal architecture. A robust in-place coal
96 seam correlation framework for the Breathitt Group (Rice and Hiett, 1994) allows sand bodies
97 to be confidently correlated from road-cut to road-cut across the basin, and lateral changes in
98 external and internal architecture within the same sand body to be assessed.

99 The Pikeville and Hyden formations of the upper Breathitt Group are the targets of this
100 study (Fig. 2). In outcrop, they contain major transversely oriented multistorey fluvial sand
101 bodies that can exceed 10 km wide, and are up to 40 m thick (Fig. 2b). Individual storeys
102 can exceed 10 m thickness, and are characterised by an erosional base overlain by a fining-
103 and thinning-upward succession dominated by trough cross bedded sandstone. However, their
104 bases are commonly lined with pebble-sized siderite clasts and peat rafts, now preserved as
105 coal, and their upper parts (if preserved) typically contain ripple cross laminated sandstone,
106 and mudstone. Architecturally, individual storeys are organised into a continuum between (i)
107 multiple fining- and thinning-upward bedsets up to 5 m thick, that display variable amounts of
108 incision into one another, and complex cross-cutting relationships, and (ii) large-scale inclined
109 bedsets (that dip by up to 15°), that extend from the base to the top of the storey, and fine
110 upward from sandstone-dominated to heterolith dominated up the inclined surface (Aitken and
111 Flint, 1994, 1995; Martino, 1996; Jerrett et al., 2017). The former are interpreted as channels
112 containing down-stream, laterally and obliquely accreting mid-channel bars, whereas the lat-
113 ter are interpreted as single-thread channels, migrating via the accretion of point-bars (Jerrett
114 et al., 2017). A minority of storeys are represented by simple basal concave-up surfaces (either
115 erosional, or representing an older topographic surface), that are passively overlapped by trough
116 cross bedded or ripple cross laminated sandstone, flaser or lenticular bedded heterolith, or shale
117 (Greb and Chesnut Jr, 1992; Aitken and Flint, 1994, 1995; Jerrett et al., 2017). Although pre-
118 dominantly interpreted as fluvial in origin, numerous workers have recognised the presence of
119 marine ichnogenera, within some storeys, especially fine-grained successions that onlap the sim-
120 ple concave-up channel-fills (e.g. Greb and Chesnut Jr, 1992; Jerrett et al., 2017). Additionally,
121 carbonaceous drapes on cross bed foresets, reversed palaeoflow readings, lenticular and flaser
122 bedding have been interpreted as tidal influence on fluvial flow in the lower reaches of some of
123 the palaeochannels (Greb and Chesnut Jr, 1992; Aitken and Flint, 1995; Martino, 1996; Jerrett
124 et al., 2017). Consequently, the role of backwater processes cannot be discounted as influencing
125 stacking patterns in these successions.

126 Regional mapping by Jerrett et al. (2017) showed that fluvial, multi-storey sand bodies
127 incised into marine strata (regional basinward shifts in facies) also have aspect ratios greater
128 than 1000, and that these represent palaeovalley fills. Some of these palaeovalleys extend from
129 the preserved orogenic to cratonic margin of the basin. Jerrett et al. (2017) interpreted these
130 as the products of the largest eustatic sea-level falls that were capable of outpacing tectonic
131 subsidence even in the most subsident parts of the preserved basin. Therefore, the preserved
132 basin (and study area) can be considered to be wholly within the “low accommodation” “Zone
133 B” in Posamentier and Allen (1993) study of the influence of subsidence patterns on stratigraphic
134 stacking patterns. By contrast Jerrett et al. (2017) demonstrated that sand bodies that show
135 no basinward facies shifts anywhere in the basin have aspect ratios that are typically less than
136 1000. Jerrett et al. (2017) recognised that these sand bodies thin, or become absent down-
137 system, and reasoned that they represent stacked successions of distributary channels which had
138 distributed their sediment load across an aggrading delta plain. These authors also recognised
139 an intermediate type of sand body with no evidence for a basinward facies shift up-dip, but
140 that do display a basinward shift in facies down-dip. These bodies have been interpreted as
141 stacked distributary channels in the up-dip higher accommodation orogenic part of the basin,
142 but pass down-dip into palaeovalleys towards the more degradational, lower accommodation
143 cratonic margin of the foreland basin. These sand bodies display intermediate aspect ratios to
144 the two other types of multistorey fluvial sand bodies (Jerrett et al., 2017) and are not targeted
145 for analysis in this study. All sand body types are extensively exposed in a series of road cuts

146 constructed throughout eastern Kentucky since the 1970s (e.g. Horne et al., 1978; Chesnut Jr,
 147 1994; Aitken and Flint, 1994; Jerrett et al., 2017). Road cuts provided exposures up to 200
 148 m high and 1 km long, but compared to the width of many of the sand bodies, irrespective of
 149 genetic type, they are often too short to provide complete cross sections through the sand bodies,
 150 capturing their complete external geometries and internal architecture. A robust in-place coal
 151 seam correlation framework for the Breathitt Group (Rice and Hiett, 1994) allows sand bodies
 152 to be confidently correlated from road-cut to road-cut across the basin, and lateral changes in
 153 external and internal architecture within the same sand body to be assessed (Fig. 2b).

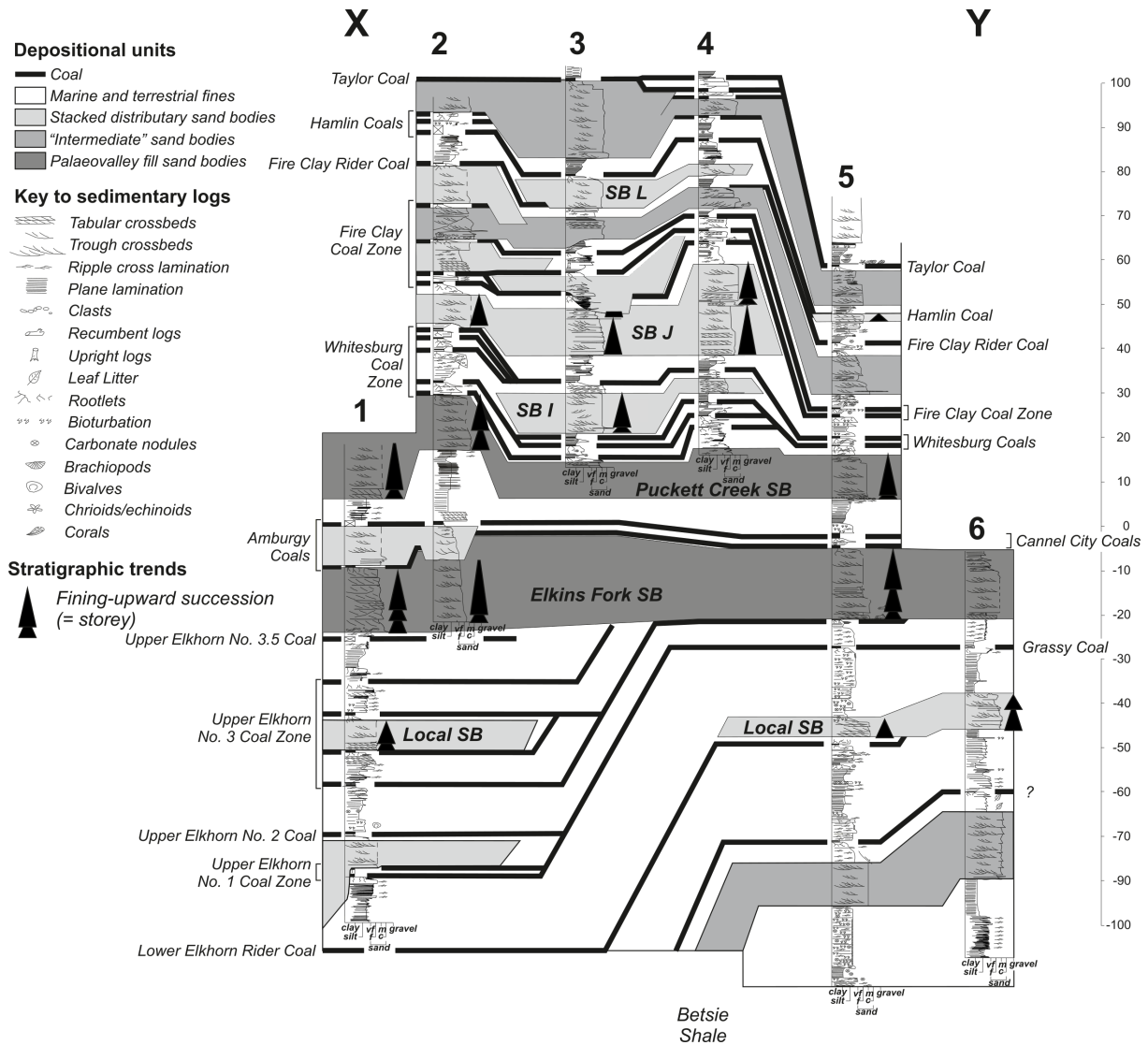


Figure 3: Correlated cross section showing sedimentary logs collected at locations 1-6. The line of section X – Y is shown of Fig. 1. Only the sand bodies characterised in this study are labelled. The locations where quantitative data were collected from these sand bodies are denoted by black triangles representing the positions of storeys within the sandstone bodies, where the sedimentary log was collected.

154 3. Methods

155 3.1. Site selection

156 Five stacked distributary channel sand bodies, and two palaeovalley fill sand bodies in the
 157 Pikeville and Hyden Formations were targeted for study at 6 locations (Fig. 1). Two of the
 158 locations are along U.S. Route 119 (US 119) between Hazard and Williamson, Pike County
 159 (Locations 1 and 2), two along Kentucky Route 7 (Ky 7) south of Hazard, Perry County (Loca-
 160 tions 3 and 4), and two along Kentucky Route 15 (Ky 15) north of Jackson, Breathitt County

161 (Locations 5 and 6; Fig. 1). Road cuts along US 119 and Ky 7 expose the Pikeville and Hyden
162 Formations approximately 40 km down depositional dip from the preserved erosional margin of
163 the basin to the SE, whereas the exposures along Ky 15 exhibit the same stratigraphy another
164 80 km down depositional dip towards the NW (Fig. 1). The sites were selected because they
165 expose the same (i.e., stratigraphically equivalent) sand bodies, which could therefore be com-
166 pared for up-to-down system differences in architecture (Fig. 3). The analysed road cuts along
167 Ky 7 are single-sided (i.e., there is exposure on just one side of the road), whereas the road cuts
168 along US 119 and Ky 15 are double-sided.

169 The stacked distributary sand bodies targeted were (a) a locally-developed unnamed sand
170 body below the Grassy Coal (at Locations 5 and 6), (b) a locally-developed unnamed sand body
171 in the Upper Elkhorn No. 3 Coal Zone (at Location 1), (c) Sand Body I (at Location 3), (d)
172 Sand Body J (at Locations 2, 3 and 4), and (e) Sand Body L (at Location 5). The palaeovalley
173 fill sand bodies targeted were the Elkins Fork Sand Body (at Locations 1, 2 and 5), and the
174 Puckett Creek Sand Body (also at Locations 1, 2 and 5). This information is summarised in
175 Table 1.

176 *3.2. Data acquisition*

177 The stratigraphy containing all targeted sand bodies at all six road cut locations was logged at
178 bed-scale, recording the full range of lithologies, grain sizes, sedimentary structures, trace and
179 body fossils. Then, a Riegl LMS-Z420i terrestrial laser scanner (TLS) was used to acquire high-
180 resolution point cloud datasets from a total swathe of each road cut. Data were collected from
181 exposures on both sides of the double-sided road cut at Locations 5 and 6 and from the single side
182 road cuts at Locations 1 and 2. Each point cloud contains a detailed 3D representation of the
183 exposures at a data point spacing of 0.05 m (~ 0.10 - 0.20 m) geometric resolution). The position
184 of each TLS location was chosen to capture as much of the exposure as possible, eliminating
185 any shadows or gaps within the data. Sub-metre DGNSS measurements were acquired for each
186 position to align them to one another at each locality, and into real world coordinates. A DSLR
187 camera was coaxially mounted on top of the scanner and used to photograph (termed "on-
188 scanner" images) the same scanned scenery, registered to its associated point cloud, creating
189 an accurate pixel-point-ratio of the datasets. Composite centimetre-scale sedimentary logs were
190 measured through the exposed stratigraphy in all six measured road cuts, providing facies and
191 palaeocurrent azimuth data, which were integrated into the finalised DOMs.

192 *3.3. Data processing*

193 Multiple software resources were used to collate, process, align and geoposition the acquired
194 data (outlined in Pringle et al., 2004; Hodgetts, 2013; Rarity et al., 2014) to produce the DOMs.
195 Each scan location position was exported into Innovmetric: PolyworksTM and integrated with
196 their associated DGNSS measurement. The alignment matrix produced from this process was
197 imported into the scan project for each locality, giving each scan location a real-world coordinate
198 position. Additionally, composite sedimentary logs were correlated and key stratigraphic and
199 architectural contacts were used to spatially define the sand bodies analysed herein.

200 *3.4. Data visualisation*

201 Once these data were collated together, a software package created at The University of Manch-
202 ester, *Virtual Reality Geological Studio* (VRGS) (Hodgetts et al., 2007), was used for visualisation
203 and analysis of high resolution, spatially accurate 3D representations of the road-cut exposures
204 (techniques outlined by van Lanen et al., 2009; Fabuel-Perez et al., 2010). The visualisation
205 method used for this study involved a photorealistic approach of colourising both point cloud
206 and surface mesh realisations from the RGB information from the on-scanner images, creating
207 a 3D photorealistic model of the scanned outcrops (Fig. 4a). A detailed description of the
208 photorealistic method applied to the models is discussed in Bellian et al. (2005); Pringle et al.
209 (2006); Fabuel-Perez et al. (2010) has been adapted for this study. These models allow for
210 identification of stratigraphic contacts and stratal architecture from the data visible only in the
211 RGB information.

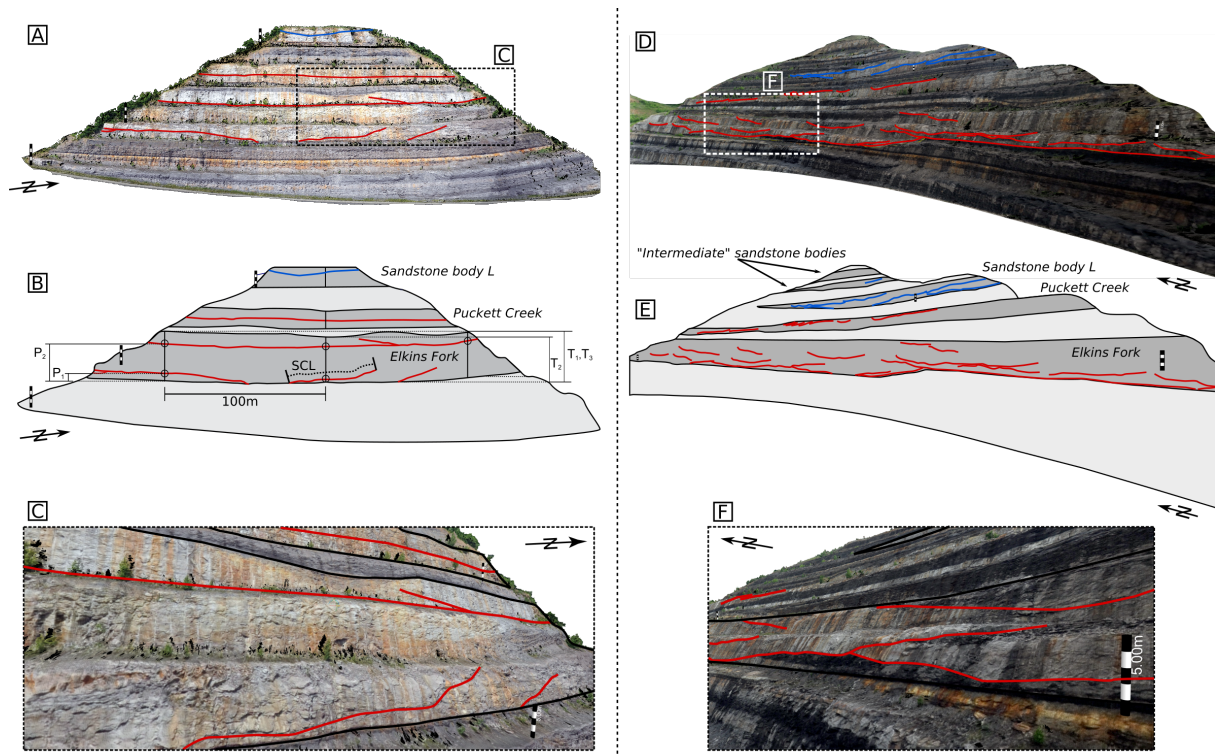


Figure 4: (A) Example of a photorealistic DOM built from integration of lidar, co-axially mounted photographic and DGNSS data illustrating a road cut at location 5 (Ky 15). (B) Illustration of how the architectural metrics were collected in each sand body. Sandstone bodies are dark grey with the internal storeys digitised in blue (stacked distributaries) and red (palaeovalleys) lines. Storey contract length (SCL), sand body thickness (T) and position of storey contact from base of sand body (P) are labelled accordingly. T and P are measured from a vertical line drawn every 100 m lateral distance (denoted by thick black lines) irrespective of the length of the exposure. For each sand body, the number of measurements taken, the mean, minimum, maximum and standard deviation are reported in Tables 1-3. (C) Detail view of 3D DOM with annotations that demarcate interpreted storey contacts within the Elkins Fork sand body. All features were interpreted in VRGS with 0.20 m spatial accuracy. *Note - scale bar is 5 m*

212 3.5. Characterisation of sand body architecture from 3D digital outcrop models

213 In this study, a sand body is referred to as a succession of sandstone channel-fill elements bounded
 214 by muddy units, irrespective of their genetic origin (i.e., stacked distributary or palaeovalley fill).
 215 Individual storeys are defined according to Friend et al. (1979) and Bridge and Tye (2000) (Fig.
 216 4b). The analytical toolset available within VRGS was used to interpret the DOMs. Sand
 217 body geometries were quantitatively described using: (a) the Polyline tool, which was used to
 218 digitise storey contacts in the three-dimensional space (Figure 4), from which the length and
 219 approximate spatial position of storey contacts could be extracted (Table 1); (b) the *Geo Polygon*
 220 tool, used to digitise a 3D polygon around each sand body, into which facies and palaeocurrent
 221 data from the sedimentary logs could be integrated, and from which the cross-sectional areas of
 222 the sand bodies could be calculated; and (c) thickness measurements were recorded by creation
 223 of 3D vertical measurements (Fig. 4b) throughout each sand body unit across the outcrops at
 224 100 m spacing in order to reduce bias where only parts of storeys are laterally preserved.

Table 1: Sand body thickness, mean position of storey contacts (from base of sand body) and storey contact lengths for stacked distributary channels and palaeovalley fills. Bulk basin-wide trends are shown, as well as trends in the up-dip proximal part of the basin (Loc. 1-4) and in the down-dip distal part of the basin (Loc. 5 and 6).

| Sand Body Name | Interpretation | Metric | Loc. 1 (US 119) | | | | | | | Loc. 2 (US 119) | | | | | | | Loc. 3 (KY 7) | | | | | | | Loc. 4 (KY 7) | | | | | | | Loc. 5 (KY 15) | | | | | | | Loc. 6 (KY 15) | | | | | | | | | | | | |
|---|----------------|-----------------------|-----------------|---------|------------|----------|---------|-----------|-------|-----------------|------------|----------|---------|-----------|----|---------|---------------|----------|---------|-----------|------|---------|------------|---------------|---------|-----------|---|---------|------------|----------|----------------|-----------|---|---------|------------|----------|---------|----------------|--|--|--|--|--|--|--|--|--|--|--|--|
| | | | N | Min (m) | Median (m) | Mean (m) | Max (m) | Std. Dev. | N | Min (m) | Median (m) | Mean (m) | Max (m) | Std. Dev. | N | Min (m) | Median (m) | Mean (m) | Max (m) | Std. Dev. | N | Min (m) | Median (m) | Mean (m) | Max (m) | Std. Dev. | N | Min (m) | Median (m) | Mean (m) | Max (m) | Std. Dev. | N | Min (m) | Median (m) | Mean (m) | Max (m) | Std. Dev. | | | | | | | | | | | | |
| L | SFC | Sand body thickness | | | | | | | | | | | | | | | | | | | | | | | | | | | | | | | | | | | | | | | | | | | | | | | | |
| | | Mean storey thickness | | | | | | | | | | | | | | | | | | | | | | | | | | | | | | | | | | | | | | | | | | | | | | | | |
| | | Storey contact length | | | | | | | | | | | | | | | | | | | | | | | | | | | | | | | | | | | | | | | | | | | | | | | | |
| J | SFC | Sand body thickness | 5 | 8.07 | 26.20 | 23.10 | 29.30 | 8.53 | 4 | 2.51 | 7.37 | 6.07 | 10.00 | 0.61 | 7 | 9.27 | 18.80 | 18.80 | 18.80 | 18.80 | 0.05 | 6.05 | | | | | | | | | | | | | | | | | | | | | | | | | | | | |
| | | Mean storey thickness | 5 | 8.00 | 9.50 | 14.25 | 14.50 | 4.60 | 4 | 5.50 | 4.41 | 5.50 | 6.00 | 0.35 | 12 | 10.00 | 10.75 | 11.25 | 13.00 | 2.12 | | | | | | | | | | | | | | | | | | | | | | | | | | | | | | |
| | | Storey contact length | 2 | 29.60 | 60.02 | 71.00 | 112.40 | 41.00 | 8 | 23.20 | 45.62 | 68.00 | 107.00 | 49.50 | 6 | 39.70 | 48.90 | 0.00 | 65.60 | 30.90 | | | | | | | | | | | | | | | | | | | | | | | | | | | | | | |
| I | SFC | Sand body thickness | | | | | | | | | | | | | | | | | | | | | | | | | | | | | | | | | | | | | | | | | | | | | | | | |
| | | Mean storey thickness | | | | | | | | | | | | | | | | | | | | | | | | | | | | | | | | | | | | | | | | | | | | | | | | |
| | | Storey contact length | | | | | | | | | | | | | | | | | | | | | | | | | | | | | | | | | | | | | | | | | | | | | | | | |
| Pocket Creek | PV | Sand body thickness | 1 | 31.3 | 41.2 | 31.3 | 31.3 | N/A | 5 | 10.00 | 10.88 | 11.00 | 13.30 | 1.29 | | | | | | | | | | | | | | | | | | | | | | | | | | | | | | | | | | | | |
| | | Mean storey thickness | 1 | 31 | 31 | 31 | N/A | 7 | 6.50 | 6.50 | 7.71 | 10.00 | 4.54 | | | | | | | | | | | | | | | | | | | | | | | | | | | | | | | | | | | | | |
| | | Storey contact length | N/A | - | - | - | - | 5 | 13.20 | 22.48 | 45.00 | 86.60 | 37.00 | | | | | | | | | | | | | | | | | | | | | | | | | | | | | | | | | | | | | |
| Elkins Fork | PV | Sand body thickness | 2 | 24.00 | 25.80 | 14.00 | 24.30 | 0.07 | 5 | 3.20 | 6.10 | 5.70 | 6.80 | 1.47 | | | | | | | | | | | | | | | | | | | | | | | | | | | | | | | | | | | | |
| | | Mean storey thickness | 3 | 8.07 | 8.00 | 10.00 | 13.00 | 0.90 | 15 | 4.00 | 3.00 | 3.55 | 7.00 | 3.54 | | | | | | | | | | | | | | | | | | | | | | | | | | | | | | | | | | | | |
| | | Storey contact length | 4 | 40.30 | 77.00 | 78.30 | 118.00 | 33.20 | 7 | 40.70 | 83.44 | 75.30 | 112.00 | 25.40 | | | | | | | | | | | | | | | | | | | | | | | | | | | | | | | | | | | | |
| Local sand body in Blount No. 3 Coal Zone | SFC | Sand body thickness | 5 | 4.12 | 0.53 | 0.63 | 8.00 | 1.73 | | | | | | | | | | | | | | | | | | | | | | | | | | | | | | | | | | | | | | | | | | |
| | | Mean storey thickness | 5 | 2.00 | 0.00 | 0.50 | 2.00 | 0.35 | | | | | | | | | | | | | | | | | | | | | | | | | | | | | | | | | | | | | | | | | | |
| | | Storey contact length | 2 | 80.20 | 83.40 | 83.40 | 86.70 | 4.58 | | | | | | | | | | | | | | | | | | | | | | | | | | | | | | | | | | | | | | | | | | |
| Local sand body below the Grassy Coal | SFC | Sand body thickness | | | | | | | | | | | | | | | | | | | | | | | | | | | | | | | | | | | | | | | | | | | | | | | | |
| | | Mean storey thickness | | | | | | | | | | | | | | | | | | | | | | | | | | | | | | | | | | | | | | | | | | | | | | | | |
| | | Storey contact length | | | | | | | | | | | | | | | | | | | | | | | | | | | | | | | | | | | | | | | | | | | | | | | | |

225 From these data the external architecture (sand body thickness) of individual sand units
226 was calculated. The mean storey thickness within each sand body was calculated. The maxi-
227 mum storey thickness approximately reflects the (undecomposed) thalweg depth of channels.
228 However, most storeys within sand bodies are truncated at their tops by incision from overlying
229 storeys, so the storey thicknesses presented represent the minimum channel depth. The position
230 of storey contacts relative to the base of each sand body was calculated, and used as a proxy
231 for the degree of storey preservation within each sand body (i.e., more storey contacts close to
232 the base of the sand body may be representative of significant erosion, and/or non-preservation
233 of earlier storeys, whereas storey contacts evenly distributed throughout the sand body may be
234 indicative of the more even preservation of storeys during deposition of the sand body). Finally,
235 the average length of individual storey contacts were calculated from the individual storey con-
236 tacts digitised and measured in each sand body. A major limitation is that, as noted by Jerrett
237 et al. (2017), many storey contacts cannot be reliably traced across the entirety of the exposure.
238 This is largely due to vegetation, masking storey contacts, or because sand-on-sand contacts
239 across storey boundaries obscure those storey contacts. Within the confines of these limitations,
240 however, individual storey contact lengths were used, and with it the number of clear discernible
241 storeys within each sand body, as a proxy for amalgamation of the sand body.

242 4. Results and discussion

243 The minimum, median, mean and maximum of each metric for the sand body thickness, mean
244 storey thickness, mean position of storeys relative to the base of the sand body, and mean length
245 of storey contacts for each measured sand body is provided in Table 1. A summary form of the
246 data organised according to whether the sand body was interpreted by Jerrett et al. (2017)
247 as a succession of stacked distributary channels or a palaeovalley is provided in Table 2 and
248 illustrated in Figures 5 and 6.

249 4.1. Comparison of stacked distributary channels and palaeovalley fills

250 Stacked distributary channel sand bodies are on average 10.7 m thick (SD = 6.8, n = 39). The
251 average thickness of their channel storeys is 6.8 m (SD = 2.4, n = 47), the mean position of
252 storey contacts inside the sand body is 5.6 m from the base of the sand body (SD = 3.5, n =
253 23), and the mean length of internal storey contacts is 65.8 m (SD = 41.0, n = 32) (Table 2).
254 Palaeovalley fills are on average 11.8 m thick (SD = 6.8, n = 24). The average thickness of their
255 channel storeys is 7.0 m (SD = 3.2, n = 35), the mean position of storey contacts inside the
256 sand body is 6.9 m from the base of the sand body (SD = 4.6, n = 20), and the mean length
257 of internal storey contacts is 60.1 m (SD = 40.3, n = 45) (Table 2). The standard deviation of
258 these data demonstrate the large overlap in these metrics between the two types of sand body
259 and therefore the limitations of using such data for discrimination between them.

260 It is possible to compare the same metrics between what we term the “up-dip domain”
261 (Locations 1-4, closer to the orogenic margin, and to the input point of the rivers into the basin)
262 and the “down-dip domain” (Locations 5 and 6, which are closer to the cratonic margin of the
263 basin and further from the input point of the rivers into the basin). The up-dip domain is also
264 an area of higher accommodation than the down-dip domain, and we purposefully use the terms
265 “higher” accommodation and “lower” accommodation” (rather than “high” and “low”) because
266 the study is entirely located within the “low accommodation” Zone B of Posamentier and Allen
267 (1993). Isopach maps for the combined Pikeville and Hyden formations (Fig. 1b) suggest that
268 accommodation rates were roughly double at higher accommodation Locations 1-4, compared to
269 lower accommodation Locations 5 and 6. In the higher accommodation up-dip domain, stacked
270 distributary channel sand bodies are, on average, thicker than palaeovalley fills (13.5 m *versus*
271 10.5 m; n = 23, n = 12). However, average storey thickness, (7.0 m in stacked distributary
272 channels, *versus* 6.8 m in palaeovalley fills; n = 33, n = 8), mean position of storey from the
273 base of the sand body (3.4 m in stacked distributary channels, *versus* 7.0 m in palaeovalley fills;
274 n = 15, n = 9), and the length of storey contacts (69.3 m in stacked distributary channels, *versus*
275 66.1 m in palaeovalley fills; n = 23, n = 16) are similar with overlapping standard deviations

Table 2: Summary of sand body thickness, mean storey thickness, mean position of storey contacts (from base of sand body), and storey contact lengths for stacked distributary channels and palaeovalley fills at up-dip locations, down-dip locations, and basin-wide. Note that most sand bodies were not analysed at all locations (see Table 1).

| Interpretation | Basin Location | Metric | N | Min | Mean | Max | Std. Dev |
|-------------------------------|-----------------------|-----------------------|-------|-------|--------|--------|----------|
| Stacked distributary channels | Up-dip | Sand body thickness | 23 | 2.51 | 13.46 | 29.30 | 7.15 |
| | | Mean storey thickness | 33 | 3.00 | 6.96 | 12.50 | 2.29 |
| | | Position of storey | 15 | 2.00 | 3.40 | 14.00 | 3.03 |
| | | Storey contact length | 23 | 23.20 | 69.34 | 167.00 | 41.00 |
| | Down-dip | Sand body thickness | 16 | 1.54 | 6.01 | 9.51 | 2.56 |
| | | Mean storey thickness | 14 | 1.00 | 5.17 | 6.00 | 2.67 |
| | | Position of storey | 8 | 1.00 | 5.17 | 7.00 | 2.76 |
| | | Storey contact length | 9 | 29.90 | 59.93 | 114.00 | 43.40 |
| | Bulk Trend | Sand body thickness | 39 | 1.54 | 10.67 | 29.30 | 6.81 |
| | | Mean storey thickness | 47 | 1.00 | 6.76 | 14.50 | 2.35 |
| | | Position of storey | 23 | 1.00 | 5.63 | 14.00 | 3.46 |
| | | Storey contact length | 32 | 23.20 | 65.81 | 167.00 | 41.00 |
| Palaeovalley fills | Up-dip | Sand body thickness | 12 | 3.29 | 10.46 | 15.30 | 3.68 |
| | | Mean storey thickness | 8 | 1.40 | 6.78 | 10.00 | 3.34 |
| | | Position of storey | 9 | 3.00 | 7.00 | 16.00 | 2.77 |
| | Down-dip | Storey contact length | 16 | 13.20 | 66.13 | 118.00 | 33.00 |
| | | Sand body thickness | 12 | 5.02 | 13.90 | 24.30 | 7.30 |
| | | Mean storey thickness | 27 | 5.90 | 8.71 | 14.00 | 1.56 |
| | | Position of storey | 11 | 1.00 | 6.75 | 16.00 | 5.30 |
| | Bulk Trend | Storey contact length | 29 | 15.50 | 50.95 | 180.00 | 44.40 |
| | | Sand body thickness | 24 | 3.29 | 11.84 | 24.30 | 6.75 |
| | | Mean storey thickness | 35 | 1.40 | 6.98 | 13.00 | 3.23 |
| Position of storey | | 20 | 1.00 | 6.90 | 16.00 | 4.63 | |
| Bulk Trend | Storey contact length | 45 | 13.20 | 60.06 | 180.00 | 40.30 | |

276 (Table 2; Fig. 5). By comparison, in the lower accommodation down-dip domain, stacked
277 distributary sand bodies are markedly thinner than palaeovalleys (6.0 m *versus* 13.9 m; n = 16,
278 n = 12). As in the up-dip domain, mean storey thickness (5.2 m in stacked distributary channels
279 *versus* 8.7 m in palaeovalley fills; n = 14, n = 27), mean position of storey contacts from the base
280 of the sand body (5.2 m in stacked distributary channels *versus* 6.8 m in palaeovalley fills; n = 8,
281 n = 11), and the length of storey contacts (59.9 m in stacked distributary channels *versus* 51.0
282 m in palaeovalley fills; n = 9, n = 29) are similar, with overlapping standard deviations (Table 2;
283 Fig. 5). The greater similarity between stacked distributary channel deposits and palaeovalley
284 fills in the up-dip domain reflects proximity to the input point of the fluvial systems into the
285 basin. Therefore, the different basinal processes associated with distributary fluvial systems and
286 valley formation and filling, as discussed below, had little opportunity to partition the two sand
287 body types into two distinct architectures.

288 4.2. Stacked distributary channel sand bodies from up-dip to down-dip

289 Stacked distributary channel sand bodies become thinner down-system, from 13.5 m to 6.0 m
290 on average (maximum 29.3 m to 15.3 m) (over c. 80 km distance; Fig. 1B). The average storey
291 thickness in these sand bodies decreases from 7.0 m to 5.17 m. Because sand body thickness
292 decreases at a greater rate than storey thickness, the average number of vertically stacked sand
293 bodies decreases from 1.9 to 1.2 down-dip. The down-dip decrease in average storey thickness
294 could reflect either a real decrease in the depth of the original channel or an increasing amount
295 of storey truncation after deposition. Two additional pieces of data suggest that the down-
296 system decrease in storey thickness in stacked distributary channels represents a real decrease in
297 the depth of the deposited channel-fills: (1) maximum measured storey thickness – the closest
298 approximation to (un-decompacted) bankfull depth of the deepest channels in the system –

299 decreases from 12.5 m up-dip, to 6 m down-dip; and (2) the down-system increase in the mean
300 position of storey contacts from 3.5 m to 5.2 m above the base of the sand body. The latter means
301 that overlying stories are less incised and amalgamated into underlying stories down-dip and that
302 the decrease in storey height is not simply a function of increased top-truncation. These data are
303 consistent with models for distributive fluvial systems in unconfined settings, where increasing
304 frictional interaction of flows with the substrate, and decreasing gradient promote rapid in-
305 channel sedimentation, superelevation of the channel above the flood plain, and channel avulsion
306 (Nichols and Fisher, 2007; Weissmann et al., 2015). Although distributive fluvial system models
307 emphasise the existence of one or few trunk distributaries at any one time (e.g. Weissmann et al.,
308 2010), avulsion is rarely instantaneous, and therefore two or more bifurcating distributaries,
309 each smaller than the upstream trunk, can coexist simultaneously. The recognition of marine
310 or brackish salinity and tidal influence in a minority of channel-fills inside the sand bodies of
311 the Pikeville and Hyden formations (e.g. Greb and Chesnut Jr, 1992; Aitken and Flint, 1995;
312 Martino, 1996; Jerrett et al., 2017) is significant to this study, because it implies that the
313 channels may have been within the reach of backwater processes (i.e., influenced by the static
314 standing body of water into which the terminal segment of river empties; e.g., Paola and Mohrig
315 (1996). Theoretical considerations (e.g. Chatanantavet et al., 2012), backed by observational
316 data from modern systems (e.g. Fernandes et al., 2016) show that in unconfined (i.e., deltaic)
317 settings, there is an increased rate of within-channel sedimentation at the transition from normal
318 (gravitationally-driven) fluvial flow to zone influenced by backwater processes (the upper 0.5 of
319 the backwater length). The high sedimentation and bar construction rates within this zone
320 drives bank erosion, lateral migration and avulsion, leading to the downstream bifurcating plan
321 view morphology of deltas, which bear superficial similarities to distributive fluvial systems.
322 The lower (i.e., downstream) 0.5 of the backwater length is characterised by relatively low
323 within-channel sedimentation rates, which conversely inhibit channel migration and avulsion.
324 Consequently long-occupied channels in fixed positions aggrade vertically. The stratigraphy
325 that results from deposits within the backwater length is a sand body that narrows and thickens
326 downstream (Fernandes et al., 2016). Palaeohydraulic analyses of channel-fills from the Pikeville
327 and Hyden formations, undertaken by Jerrett et al. (2017) suggest that these fluvial systems
328 may have had backwater lengths in the order of 40-220 km, but because the contemporaneous
329 shorelines to these fluvial sandstones have not been recognised, it is difficult to have any sense
330 of the position of the transition from normal fluvial flow to backwater influenced. Certainly,
331 the down-system decrease in sand body thickness recorded within stacked distributary channel
332 sand bodies, imply that backwater processes, if present within the study area at all, were less
333 important than continental distributive fluvial processes. The combination of the down-system
334 decrease in sand body and storey thickness, with the decreased number of vertically stacked
335 storeys are a function of decreasing channel depths, and a concomitant decrease in confinement
336 and amalgamation of the original channels that is characteristic of distributive fluvial systems
337 (Davidson et al., 2013; Weissmann et al., 2013).

338 The lengths of storey contacts inside the sand bodies vary from 69.3/100 m up-dip, to
339 59.9/100 m down-dip. Storey contacts form as a channel migrates across and erodes into a
340 flood- or delta-plain. Lateral or downstream accreting bars downlap the erosion surface and de-
341 posit a channel belt or storey that has a much greater aspect ratio than the channel that formed
342 it Miall (1985); Gibling (2006). Primary factors that influence the length of time, or rate of lat-
343 eral migration of a channel, that will therefore influence the length of a storey contact include:
344 (a) the channel morphology and fluvial style in which high sinuosity channels typically display
345 higher rates of lateral migration and lower rates of avulsion than low sinuosity channels (Schumm
346 et al., 1996); (b) substrate strength (Stouthamer and Berendsen, 2000; Aslan et al., 2005); and
347 (c) rate of accommodation generation, with higher rates of accommodation promoting vertical
348 aggradation, sedimentation and frequent avulsion (Bridge and Leeder, 1979; Bryant et al., 1995;
349 Blum and Törnqvist, 2000; Slingerland and Smith, 2004; Aslan et al., 2005). The self-similar
350 behaviour of channels dictates that, all other factors being equal, a larger channel will migrate
351 a greater distance before avulsing, and will therefore generate a longer storey contact (Nanson

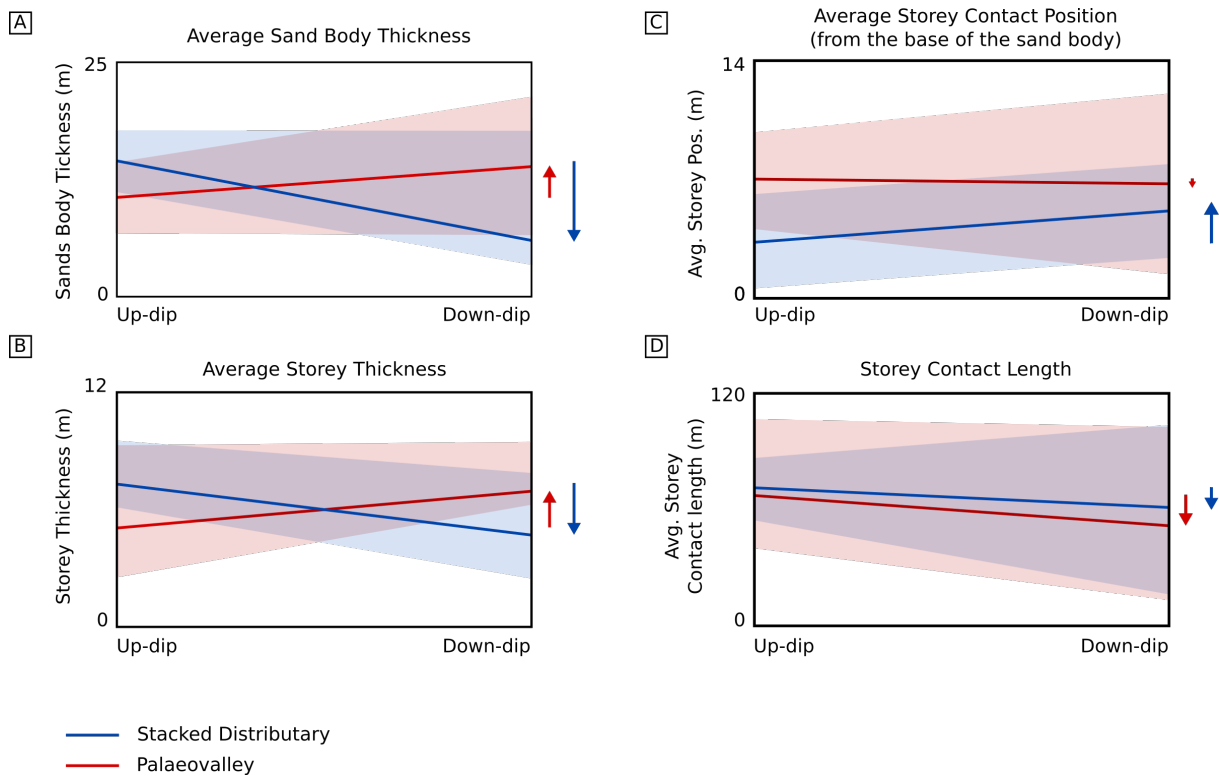


Figure 5: Plot depicting changes in the architectural metrics from up-system to down-system in stacked distributary channel sand bodies (blue) from palaeovalley fill (red) sandstone bodies. Standard deviations for each metric and the associated up-system to down-system changes in sand body type are represented by the associated shaded regions (*blue* = stacked distributary channel sand bodies; *red* = palaeovalley sand bodies). Arrows indicate approximate up-dip to down-dip changes for each metric.

352 and Hickin, 1986; Richard et al., 2005). Lengths of preserved storeys are also a function of their
 353 truncation during channel amalgamation, with reduced length indicative of greater truncation
 354 and storey amalgamation. Although a general decrease down-dip in grain size has been identified
 355 in the system (Jerrett et al., 2017), no systematic change in fluvial style down-system has been
 356 recognised, which could otherwise influence bank mobility and the lengths of storey contacts.
 357 Because this study only takes into account internal storey contacts, the substrate into which
 358 all the contacts was eroded was in each case fluvial sand of the underlying sand body. In this
 359 foreland basin setting, where fluvial systems prograded from a zone of higher accommodation
 360 on the orogenic margin, to a zone of lower accommodation on the cratonic margin, decreasing
 361 storey contacts down-system are not consistent with accommodation being the primary control
 362 on this metric. Finally, the down-system decrease in the number of vertically stacked channels
 363 and increase in vertical aggradation argues for reduced, not increased, down-system erosion and
 364 amalgamation. Therefore, the down-system reduction in storey contact lengths in stacked dis-
 365 tributary channels are interpreted to be a function of the down-system decrease in channel size.
 366 Overall, the data demonstrate that stacked distributive sand bodies decrease in thickness down-
 367 system, primarily driven by a down-system decrease in channel size, consistent with unconfined
 368 avulsive processes typical of distributive fluvial systems (Hartley et al., 2010; Davidson et al.,
 369 2013). Though the concept, and plan-view characteristics of distributive fluvial systems were
 370 defined explicitly for fully continental (i.e., non-deltaic) systems (Hartley et al., 2010; Weiss-
 371 mann et al., 2015) the down-system decrease in vertical channel amalgamation and increase in
 372 vertical aggradation reflects deconfinement and radiation of distributary channels away from
 373 major entry points into the basin (Nichols and Fisher, 2007; Hartley et al., 2010; Weissmann
 374 et al., 2015). Therefore, these architectures would be fully expected in, and the methods of
 375 recognising them are exportable to the continental settings envisaged by Hartley et al. (2010)
 376 and Weissmann et al. (2015).

377 4.3. Palaeovalley sandstone bodies from up-dip to down-dip

378 Palaeovalley sand bodies become thicker down-system, from 10.5 m to 13.9 m, on average. The
 379 average storey thickness in these sand bodies increases, therefore the number of vertically stacked
 380 sand bodies also increases from 1.5 to 1.6 down-dip. The fact that (1) maximum storey thickness
 381 – the parameter most indicative of channel bankfull depth – increases down-system from 10.0 m
 382 to 14.0 m (over c. 80 km), and (2) the average position of storey contacts from the base of the
 383 sand bodies decreases from 7.0 m to 6.8 m, are indicative that the down-system increase in storey
 384 height is a result of an increase in channel size down-system, rather than because of reduced
 385 down-system channel amalgamation. Overall, then, the data suggest that in palaeovalley fills,
 386 the sand bodies become thicker down-system, and that this is associated with a down-system
 387 increase in the original channel sizes. This trend is accompanied by a modest down-system
 388 increase in the number of vertically stacked storeys and channel truncation and amalgamation.

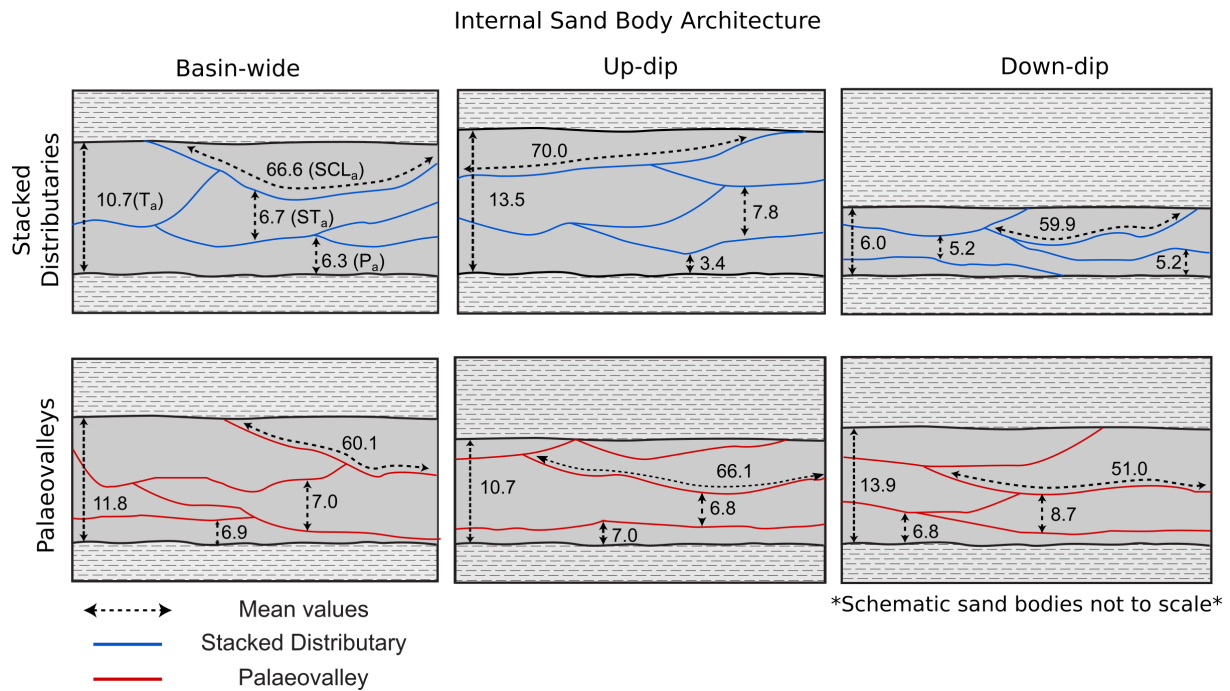


Figure 6: Schematic illustrating the basin-wide, up-dip and down-dip architectures of stacked distributary channel-fill and palaeovalley fill sandstone bodies. Abbreviations: The average sand body thickness (T_a), average storey thickness (ST_a), average position of storey contact relative to base of sand body (P_a), and average storey contact length (SCL_a) are drawn relative to one another. sandstone bodies are not to scale and are only relative to one another.

389 The down-system increase in bankfull depths in the sand bodies that display a basinward
 390 facies shift at their base is wholly compatible with existing models for valley formation and
 391 filling. Valleys form in sedimentary basins when an increase in stream power allows the flu-
 392 vial system to re-entrain previously deposited sediments, or erode into underlying bedrock, as
 393 the system adjusts to a new equilibrium surface which is lower than the previous one (Bhat-
 394 tacharya, 2011; Holbrook et al., 2006; Posamentier and Vail, 1988). This increase in stream
 395 power is often associated with increased gradient in response to lowered eustatic sea-level or
 396 tectonic uplift, but can also occur because of increased discharge and changes in sediment cali-
 397 bre (Blum and Törnqvist, 2000; Holbrook et al., 2006). The change from deposition to erosion
 398 is associated with the formation of new geomorphic elements: the development of a tributive
 399 fluvial network, headwardly-migrating erosional knickpoints, which can intercept and capture
 400 neighbouring fluvial systems (Bhattacharya, 2011; Van Heijst and Postma, 2001; Wescott, 1993).
 401 Stream capture, in particular, will increase fluvial discharge down-system, and substantially in-
 402 crease the capacity of the system to erode into the underlying substrata. As discussed by Blum
 403 et al. (2013), valley formation is not associated with erosion alone, and terraces of channel belts
 404 and associated floodplain strata are typically deposited and preserved within the confines of

405 the valley during fluvial incision. Those channel belts deposited during degradational valley-
406 forming phases should display storey thicknesses that increase down-system. Palaeovalley fills
407 include also the deposits within the valley that are formed during subsequent aggradational
408 back-filling, this time as a response to decreasing fluvial power and capacity of the system to
409 transport and erode sediment. The antecedent tributive network of streams generated during
410 degradation and initial valley formation will persist (and continue to erode) until the entirety
411 of the accommodation excess in the valley is filled (Blum et al., 2013). Hence, channel belts
412 deposited during the aggradational valley healing phase will also display storey thicknesses that
413 increase down-system.

414 The increase in the number of stacked stories, and channel-fill amalgamation is likely a
415 function of the tectonic setting of these transverse palaeovalley sand bodies in the central Ap-
416 palachian foreland basin. In foreland basins, there is a higher rate of tectonic subsidence towards
417 the orogenic margin, compared to the cratonic margin. Consequently, during palaeovalley for-
418 mation, the higher rates of tectonic accommodation in the up-dip, orogenic margin will suppress
419 the degree of erosion and amalgamation into underlying deposits. Towards the cratonic mar-
420 gin, a lower rate of tectonic accommodation will promote truncation and amalgamation of the
421 channel-fills as the fluvial system cuts and fills the valley (Jerrett et al., 2017). This architec-
422 tural motif in the palaeovalleys of the Pikeville and Hyden formations – increased truncation and
423 amalgamation down-system – is likely more characteristic of the tectonic setting, rather than
424 inherent to palaeovalley systems in general (cf., passive margins where accommodation increases
425 down-system).

426 At first glance, the down-dip decrease in the mean lengths of storey contacts in palaeovalley
427 fills from 66.1 m to 51.0 m is counter-intuitive, given that down-system decreases in lengths
428 of storey contacts in stacked distributary channel deposits were ascribed to decreasing channel
429 size. This decrease may be related to a down-system increase in confinement of the channels
430 within more mature palaeovalleys, which inhibited lateral accretion, and formation of long storey
431 contacts.

432 5. Conclusions

433 This study demonstrates that stacked distributary channels and palaeovalley fills exhibit differ-
434 ent basin-scale architectures. These differences can be difficult to identify from outcrop data,
435 especially close to the input point of fluvial systems into the sedimentary basin. The principal
436 control on stacked distributary channel architecture is the regional down-system avulsion be-
437 haviour and reduction in confinement of distributive fluvial systems, which result in down-system
438 decreases in channel size and channel amalgamation. This in turn results in sand bodies that thin
439 down system, storeys that reduce in thickness, storey contacts that increase in their positions in
440 the sand body, and storey contacts that reduce in length. The principal control on palaeovalley
441 fill architecture is the down-system tributive nature of the fluvial systems that deposit during
442 both the degradational valley-forming phase, and aggradational valley-filling phase. Channels
443 increase in size down-dip, resulting in sand bodies and storeys that thicken down-system. A
444 secondary control on palaeovalley architecture is the regional accommodation profile. In the
445 Central Appalachian Basin, a down-system decrease in tectonic accommodation, from the oro-
446 genic margin towards the foreland resulted in increased channel amalgamation down-system,
447 with the effect of reducing the mean position of storey contacts inside the resulting sand bodies.
448 This tectonic control would be likely reversed in passive margin basins, where accommodation
449 increases down the fluvial system. Regional accommodation is a strong influence on the archi-
450 tectures of both stacked distributary channels and palaeovalleys in other basin settings, so the
451 results of this study should not be universally applied without consideration of basin setting
452 and the scale of the fluvial systems operating in the basin. Another consideration influencing
453 down-system stratal architectures will be the possible influence of backwater processes where
454 fluvial systems enter lakes or the sea.

455
456

457 **Acknowledgements**

458

459 The authors thank and acknowledge Total S.A. for funding the research that lead to the presented
460 work. The authors would like to further thank Georgina Heldreich and Rachel Harding for
461 providing useful comments on an early draft of the manuscript. Finally the authors kindly and
462 appreciatively thank and acknowledge Janok Bhattacharya and an anonymous reviewer, and
463 Chief Editor Jasper Knight for their constructive reviews and feedback

464 **References**

- 465 Aitken, J. F. and Flint, S. S. (1994). High-Frequency Sequences and the Nature of Incised-Valley
466 Fills in Fluvial Systems of the Breathitt Group (Pennsylvanian), Appalachian Foreland Basin,
467 Eastern Kentucky.
- 468 Aitken, J. F. and Flint, S. S. (1995). The application of high-resolution sequence stratigraphy to
469 fluvial systems: a case study from the upper carboniferous breathitt group, eastern kentucky,
470 usa. *Sedimentology*, 42(1):3–30.
- 471 Aslan, A., Autin, W. J., and Blum, M. D. (2005). Causes of river avulsion: insights from the
472 late holocene avulsion history of the mississippi river, usa. *Journal of Sedimentary Research*,
473 75(4):650–664.
- 474 Bellian, J. A., Kerans, C., and Jennette, D. C. (2005). Digital outcrop models: applications
475 of terrestrial scanning lidar technology in stratigraphic modeling. *Journal of sedimentary
476 research*, 75(2):166–176.
- 477 Bhattacharya, J. P. (2011). Practical problems in the application of the sequence stratigraphic
478 method and key surfaces: integrating observations from ancient fluvial–deltaic wedges with
479 quaternary and modelling studies. *Sedimentology*, 58(1):120–169.
- 480 Blum, M., Martin, J., Milliken, K., and Garvin, M. (2013). Paleovalley systems: insights from
481 quaternary analogs and experiments. *Earth-Science Reviews*, 116:128–169.
- 482 Blum, M. D. and Törnqvist, T. E. (2000). Fluvial responses to climate and sea-level change: a
483 review and look forward. *Sedimentology*, 47:2–48.
- 484 Bridge, J. S. and Leeder, M. R. (1979). A simulation model of alluvial stratigraphy. *Sedimen-
485 tology*, 26(5):617–644.
- 486 Bridge, J. S. and Tye, R. S. (2000). Interpreting the dimensions of ancient fluvial channel bars,
487 channels, and channel belts from wireline-logs and cores. *AAPG bulletin*, 84(8):1205–1228.
- 488 Bryant, M., Falk, P., and Paola, C. (1995). Experimental study of avulsion frequency and rate
489 of deposition. *Geology*, 23(4):365–368.
- 490 Buckley, S. J., Howell, J., Enge, H., and Kurz, T. (2008). Terrestrial laser scanning in geology:
491 data acquisition, processing and accuracy considerations. *Journal of the Geological Society*,
492 165(3):625–638.
- 493 Burnham, B. S. and Hodgetts, D. (2018). Quantifying spatial and architectural relationships
494 from fluvial outcrops. *Geosphere*, 15(1):236–253.
- 495 Chatanantavet, P., Lamb, M. P., and Nittrouer, J. A. (2012). Backwater controls of avulsion
496 location on deltas. *Geophysical Research Letters*, 39(1).
- 497 Chesnut Jr, D. R. (1994). Eustatic and tectonic control of deposition of the lower and middle
498 pennsylvanian strata of the central appalachian basin.
- 499 Davidson, S. K., Hartley, A. J., Weissmann, G. S., Nichols, G. J., and Scuderi, L. A. (2013).
500 Geomorphic elements on modern distributive fluvial systems. *Geomorphology*, 180:82–95.
- 501 Fabuel-Perez, I., Hodgetts, D., and Redfern, J. (2010). Integration of digital outcrop models
502 (doms) and high resolution sedimentology-workflow and implications for geological modelling:
503 Oukaimeden sandstone formation, high atlas (morocco). *Petroleum Geoscience*, 16(2):133–
504 154.

- 505 Fernandes, A. M., Törnqvist, T. E., Straub, K. M., and Mohrig, D. (2016). Connecting the back-
506 water hydraulics of coastal rivers to fluvio-deltaic sedimentology and stratigraphy. *Geology*,
507 44(12):979–982.
- 508 Friend, P., Slater, M., and Williams, R. (1979). Vertical and lateral building of river sandstone
509 bodies, ebro basin, spain. *Journal of the Geological Society*, 136(1):39–46.
- 510 Gibling, M. R. (2006). Width and thickness of fluvial channel bodies and valley fills in the
511 geological record: a literature compilation and classification. *Journal of sedimentary Research*,
512 76(5):731–770.
- 513 Gradstein, F. M., Ogg, J. G., Schmitz, M., and Ogg, G. (2012). *The geologic time scale 2012*.
514 elsevier.
- 515 Greb, S. F. and Chesnut Jr, D. R. (1992). Transgressive channel filling in the breathitt formation
516 (upper carboniferous), eastern kentucky coal field, usa. *Sedimentary geology*, 75(3-4):209–221.
- 517 Greb, S. F., Pashin, J. C., Martino, R. L., and Eble, C. F. (2008). Appalachian sedimentary
518 cycles during the pennsylvanian: Changing influences of sea level, climate, and tectonics.
519 *Resolving the Late Paleozoic Ice Age in Time and Space*, 441:235.
- 520 Hampson, G., Davies, S., Elliott, T., Flint, S., and Stollhofen, H. (1999). Incised valley fill
521 sandstone bodies in upper carboniferous fluvio–deltaic strata: recognition and reservoir char-
522 acterization of southern north sea analogues. In *Geological Society, London, Petroleum Geology*
523 *Conference series*, volume 5, pages 771–788. Geological Society of London.
- 524 Hartley, A. J., Weissmann, G. S., Nichols, G. J., and Warwick, G. L. (2010). Large distribu-
525 tive fluvial systems: characteristics, distribution, and controls on development. *Journal of*
526 *Sedimentary Research*, 80(2):167–183.
- 527 Hirst, J. (1992). Variations in alluvial architecture across the oligo-miocene huesca fluvial system,
528 ebro basin, spain.
- 529 Hodgetts, D. (2013). Laser scanning and digital outcrop geology in the petroleum industry: A
530 review. *Marine and Petroleum Geology*, 46:335–354.
- 531 Hodgetts, D., Gawthorpe, R., Wilson, P., and Rarity, F. (2007). Integrating digital and tradi-
532 tional field techniques using virtual reality geological studio (vrgs). In *69th EAGE Conference*
533 *and Exhibition incorporating SPE EUROPEC 2007*.
- 534 Holbrook, J., Scott, R. W., and Oboh-Ikuenobe, F. E. (2006). Base-level buffers and buttresses:
535 a model for upstream versus downstream control on fluvial geometry and architecture within
536 sequences. *Journal of Sedimentary Research*, 76(1):162–174.
- 537 Holbrook, J. M. and Bhattacharya, J. P. (2012). Reappraisal of the sequence boundary in time
538 and space: case and considerations for an su (subaerial unconformity) that is not a sediment
539 bypass surface, a time barrier, or an unconformity. *Earth-Science Reviews*, 113(3-4):271–302.
- 540 Horne, J., Ferm, J., Caruccio, F., and Baganz, B. (1978). Depositional models in coal exploration
541 and mine planning in appalachian region. *AAPG bulletin*, 62(12):2379–2411.
- 542 Jennette, D. C., Jones, C. R., Van Wagoner, J. C., and Larsen, J. E. (1991). High-resolution
543 sequence stratigraphy of the upper cretaceous tocito sandstone: the relationship between
544 incised valleys and hydrocarbon accumulation, san juan basin, new mexico.
- 545 Jerrett, R. M., Flint, S. S., and Brunt, R. L. (2017). Palaeovalleys in foreland ramp settings:
546 what happens as accommodation decreases down dip? *Basin Research*, 29(6):747–774.

- 547 Kukulski, R. B., Hubbard, S. M., Moslow, T. F., and Raines, M. K. (2013). Basin-scale strati-
548 graphic architecture of upstream fluvial deposits: Jurassic–cretaceous foredeep, alberta basin,
549 canada. *Journal of Sedimentary Research*, 83(8):704–722.
- 550 Martino, R. (1996). Stratigraphy and depositional environments of the kanawha formation
551 (middle pennsylvanian), southern west virginia, usa. *International Journal of Coal Geology*,
552 31(1-4):217–248.
- 553 Miall, A. D. (1985). Architectural-element analysis: a new method of facies analysis applied to
554 fluvial deposits. *Earth-Science Reviews*, 22(4):261–308.
- 555 Nanson, G. C. and Hickin, E. J. (1986). A statistical analysis of bank erosion and channel
556 migration in western canada. *Geological Society of America Bulletin*, 97(4):497–504.
- 557 Nichols, G. and Fisher, J. (2007). Processes, facies and architecture of fluvial distributary system
558 deposits. *Sedimentary geology*, 195(1-2):75–90.
- 559 Olariu, M. I., Aiken, C., Bhattacharya, J., and Xu, X. (2011). Interpretation of channelized
560 architecture using three-dimensional photo real models, pennsylvanian deep-water deposits at
561 big rock quarry, arkansas. *Marine and Petroleum Geology*, 28(6):1157–1170.
- 562 Owen, A., Nichols, G. J., Hartley, A. J., Weissmann, G. S., and Scuderi, L. A. (2015). Quan-
563 tification of a distributive fluvial system: the salt wash dfs of the morrison formation, sw usa.
564 *Journal of Sedimentary Research*, 85(5):544–561.
- 565 Paola, C. and Mohrig, D. (1996). Palaeohydraulics revisited: Palaeoslope estimation in coarse-
566 grained braided rivers. *Basin Research*, 8(3):243–254.
- 567 Posamentier, H. and Vail, P. (1988). Eustatic controls on clastic deposition ii—sequence and
568 systems tract models.
- 569 Posamentier, H. W. and Allen, G. P. (1993). Variability of the sequence stratigraphic model:
570 effects of local basin factors. *Sedimentary geology*, 86(1-2):91–109.
- 571 Pringle, J., Howell, J., Hodgetts, D., Westerman, A., and Hodgson, D. (2006). Virtual outcrop
572 models of petroleum reservoir analogues: a review of the current state-of-the-art. *First break*,
573 24(3):33–42.
- 574 Pringle, J., Westerman, A., Clark, J., Drinkwater, N., and Gardiner, A. (2004). 3d high-
575 resolution digital models of outcrop analogue study sites to constrain reservoir model uncer-
576 tainty: an example from alport castles, derbyshire, uk. *Petroleum Geoscience*, 10(4):343–352.
- 577 Quinlan, G. M. and Beaumont, C. (1984). Appalachian thrusting, lithospheric flexure, and the
578 paleozoic stratigraphy of the eastern interior of north america. *Canadian Journal of Earth
579 Sciences*, 21(9):973–996.
- 580 Rarity, F., Van Lanen, X., Hodgetts, D., Gawthorpe, R., Wilson, P., Fabuel-Perez, I., and
581 Redfern, J. (2014). Lidar-based digital outcrops for sedimentological analysis: workflows and
582 techniques. *Geological Society, London, Special Publications*, 387(1):153–183.
- 583 Rice, C. L. and Hiett, J. K. (1994). Revised correlation chart of coal beds, coal zones, and
584 key stratigraphic units in the pennsylvanian rocks of eastern kentucky. Technical report, US
585 Geological Survey.
- 586 Richard, G. A., Julien, P. Y., and Baird, D. C. (2005). Statistical analysis of lateral migration
587 of the rio grande, new mexico. *Geomorphology*, 71(1-2):139–155.
- 588 Slingerland, R. and Smith, N. D. (2004). River avulsions and their deposits. *Annu. Rev. Earth
589 Planet. Sci.*, 32:257–285.

- 590 Stouthamer, E. and Berendsen, H. J. (2000). Factors controlling the holocene avulsion history of
591 the rhine-meuse delta (the netherlands). *Journal of Sedimentary Research*, 70(5):1051–1064.
- 592 Tankard, A. J. (1986). Depositional response to foreland deformation in the carboniferous of
593 eastern kentucky. *AAPG Bulletin*, 70(7):853–868.
- 594 Thomas, W. A. (1976). Evolution of ouachita-appalachian continental margin. *The Journal of*
595 *Geology*, 84(3):323–342.
- 596 Van Heijst, M. and Postma, G. (2001). Fluvial response to sea-level changes: a quantitative
597 analogue, experimental approach. *Basin Research*, 13(3):269–292.
- 598 van Lanen, X. M., Hodgetts, D., Redfern, J., and Fabuel-Perez, I. (2009). Applications of digital
599 outcrop models: two fluvial case studies from the triassic wolfville fm., canada and oukaïmeden
600 sandstone fm., morocco. *Geological Journal*, 44(6):742–760.
- 601 Van Wagoner, J., Posamentier, H., Mitchum, R., Vail, P., Sarg, J., Loutit, T., and Hardenbol,
602 J. (1988). An overview of the fundamentals of sequence stratigraphy and key definitions.
- 603 Van Wagoner, J. C., Mitchum, R., Champion, K., and Rahmanian, V. (1990). Siliciclastic se-
604 quence stratigraphy in well logs, cores, and outcrops: concepts for high-resolution correlation
605 of time and facies.
- 606 Weissmann, G., Hartley, A., Nichols, G., Scuderi, L., Olson, M., Buehler, H., and Banteah, R.
607 (2010). Fluvial form in modern continental sedimentary basins: distributive fluvial systems.
608 *Geology*, 38(1):39–42.
- 609 Weissmann, G., Hartley, A., Scuderi, L., Nichols, G., Davidson, S., Owen, A., Atchley, S.,
610 Bhattacharyya, P., Chakraborty, T., Ghosh, P., et al. (2013). Prograding distributive fluvial
611 systems: geomorphic models and ancient examples. *New Frontiers in Paleopedology and*
612 *Terrestrial Paleoclimatology: SEPM, Special Publication*, 104:131–147.
- 613 Weissmann, G., Hartley, A. J., Scuderi, L., Nichols, G., Owen, A., Wright, S., Felicia, A.,
614 Holland, F., and Anaya, F. (2015). Fluvial geomorphic elements in modern sedimentary basins
615 and their potential preservation in the rock record: a review. *Geomorphology*, 250:187–219.
- 616 Wescott, W. (1993). Geomorphic thresholds and response of fluvial systems - implications for
617 sequence stratigraphy. *AAPG Bulletin*, 77:1208–1218.
- 618 Wu, C. and Bhattacharya, J. (2015). Paleohydrology and 3d facies architecture of ancient point
619 bars , ferron sandstone, notom delta, south-central utah. *Journal of, Sedimentary Research*,
620 85:399–418.